Ultra High-speed Photodetectors and Photoreceivers for Telecom and Datacom also Aiming at THz Applications

Heinz-Gunter Bach
Fraunhofer Institute for Telecommunications, Heinrich-Hertz-Institut, Einsteinufer 37,
D-10587 Berlin, Germany, Phone: ++49(0)30 31002-503, Fax: ++49(0)30 31002-558,
e-mail: bach@hhi.fraunhofer.de

Abstract: *Ultra-high speed photodetectors and receivers based on advanced waveguide-integrated photodiodes are presented. Main applications are the up-coming 100 G Ethernet and optical free space communications. The waveguide-integrated InP-based detectors are monolithically integrated with HEMTs, employing semi-insulating optical waveguides on a semi-insulating InP:Fe substrate, leading to 80/85 Gbit/s photoreceivers. For serving the emerging THz sensor and security application fields, a monolithic integration of a micro-pin photodiode with a circularly-toothed planar logarithmic-periodic antenna is presented and analysed in the 100 GHz range.*

Introduction

Leading system providers upgrade their long-haul optical communication systems for single channel bit rates of 40 Gbit/s, aiming to exploit the transport capacities of the single-mode fiber (SMF) of exceeding 10 Tbit/s by joint progress in combining time division multiplexing (TDM) and wavelength division multiplexing (WDM) techniques. System developers push experiments employing 80/85 Gbit/s data rates with the aim to proceed towards serial PHY 100 G Ethernet solutions and to support optical data transmission rates even at e.g. 160 Gbit/s and higher [1], to serve the steadily increasing data traffic (Fig. 1).

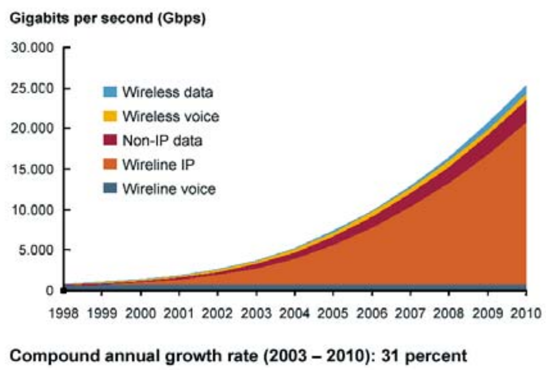

Fig. 1: Ever increasing data traffic;
source: IST Concertation Meeting September 2004.

FhG-HHI developed a family of 40 to 160 Gbit/s photodetectors and receivers, focussed on various high-power waveguide-integrated photodiodes, including those of special structure (twin-type, balanced or traveling wave) and InP-based monolithically integrated pinTWA photoreceivers (OEIC receiver) for 40/43 and 80/85 Gbit/s data rates [2, 3]. Those developments are based on a flexible integration concept, using semi-insulating substrates and semi-insulating optical waveguide layer stacks. Based on the waveguide-integrated concept, in section 1 high-power ultra-broadband photodetectors approaching a 3 dB cut-off frequency of 110 GHz are presented including their packaging into pig-tailed modules. In section 2 photoreceiver concepts are discussed, leading to the distributed amplifier type for achieving highest speed in electronic amplification. The receiver integration concept will be explained, which allows the monolithic integration of waveguides, MMI splitters, evanescently coupled pin photodiodes, HEMTs and distributed amplifiers. An advanced ultra-broadband pinTWA receiver OEIC for 80/85 Gbit/s detection is presented. The detectors and photoreceivers described are suitable for electrical TDM (ETDM) with high data rates (actually up to 160 Gbit/s in case of the detectors) within the single channel as well as for even higher data rates in transmission schemes employing optical TDM (OTDM) techniques. In section 3 the waveguide-integrated photodiodes are miniaturized into micro-pin photodiodes. These are then monolithically integrated with a circularly-toothed planar logarithmic-periodic antenna to represent a transmitter chip, aiming at THz applications.

1. Photodiodes and Modules for 100 G Ethernet

Side-illuminated photodetectors show an improved high-power behaviour, because the absorption is distributed laterally into a larger length of a thinner absorption layer in a controlled manner, compared to perpendicular illuminated detectors. Our waveguide-integrated photodiode employs a rib-waveguide, the light from which is coupled evanescently from the lower side into the small-gap absorption layer. This type of detector comprises also a monolithic taper at its input waveguide facet.
The recently fabricated photodetector chips are based on InP and comprise an evanescently coupled mesa photodiode of 5x20 μm^2 size, a spot-size converter for increased fiber alignment tolerances, a biasing network and a 50 Ω matching resistor. An optimized impedance line connecting the p-mesa to the electrical output line of the detector leads to an increase of the cut-off frequency up to 110 GHz [4].

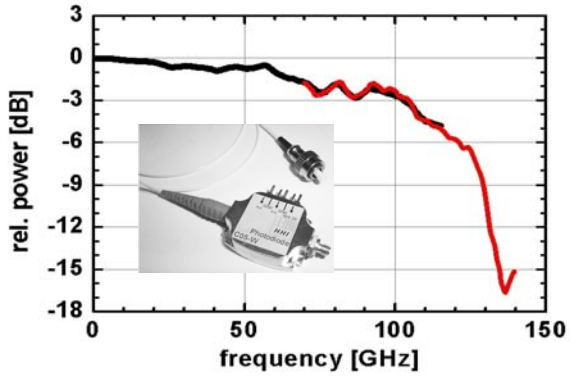

Fig. 2: Relative frequency response of the PD module (+2.3 dBm optical input power) measured with hp437B (black) and PM3 (red) , inset: photograph of the PD module.

The chip is assembled into a housing equipped with a 1 mm coaxial output connector and a fiber pigtail (Fig. 2, inset). A cleaved fiber is fixed directly at the chip's antireflection-coated waveguide facet. A responsivity of 0.73 A/W with a polarization dependent loss (PDL) of only 0.4 dB at 1.55 µm wavelength was obtained. The electrical output signal is provided by a short coplanar waveguide (CPW) which is connected by multiple short bonding wires to a following low-loss CPW on quartz substrate leading to the output connector. All fabricated modules are routinely tested for robustness against vibration (10 min, 60 g, 50 Hz) and thermal cycling from 10°C to 50°C and showed no degradation. The frequency characteristic of the photodetector (PD) module was determined by an optical heterodyne measurement setup employing a fixed and a tunable laser around 1.55 µm. The RF signal was measured by a power meter (hp437B) with three different power sensors for the respective RF bands 0-50 GHz, V- and W-band. In the F-band (90-140 GHz) we used a high-frequency power meter (PM3 Erickson Instr.). An excellent agreement of the measured characteristics was observed in the overlapping frequency ranges. Fig. 2 shows the calibrated frequency response of the photodetector module at 2 V reverse bias (V_{bias}). A -3 dB bandwidth of 100 GHz is obtained. At 120 GHz signal frequency

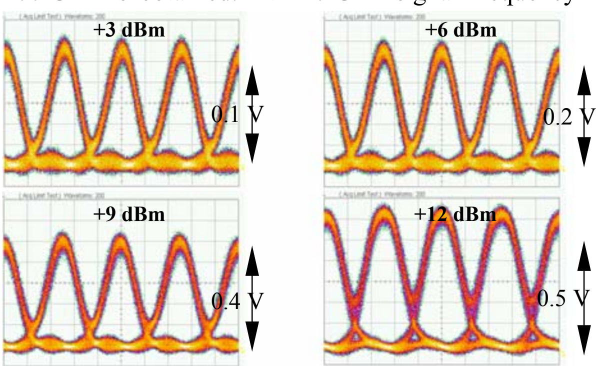

Fig. 3 Electrical 80 Gbit/s RZ eye pattern at 3, 6, 9 and 12 dBm optical input power detected by the detector module at -2.5 V bias (x: 5ps/div).

the response has decreased by 6 dB. The dip around 135 GHz can be attributed to a higher order mode arising in the coaxial connector, which limits the performance of the 1 mm coaxial interface.

Mounting alternatives comprising flip-chip technology led to similar good broadband properties.

The PD modules have been evaluated in several back-to-back OTDM transmission experiments.

Fig. 3 shows the received electrical 80 Gbit/s RZ eye patterns at different optical input power levels using the setup described in [5]. All measured eye patterns are opened widely with a peak voltage up to 0.6 V revealing only negligible saturation effects at +12 dBm.

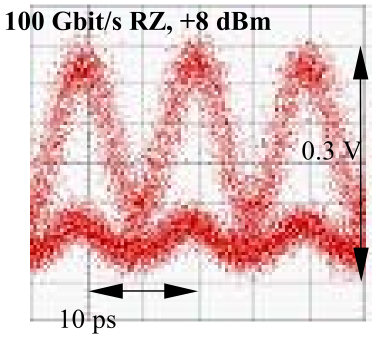

Fig. 4 100 Gbit/s RZ eye pattern at +8 dBm input power, V_{bias}: -2 V, 2^{20}-1 PRBS (courtesy of L. Moeller, Lucent Techn., USA).

Measurements at 100 Gbit/s RZ were performed using a 100 GHz sampling scope (LeCroy SDA with SE-100 standard time base) demonstrating the highest available bit rate with RZ modulation format at which o/e conversion could be performed without any reduction of the modulation depth (Fig. 4).

Fig. 5 shows the detected 160 Gbit/s RZ data stream at +12 dBm optical input power. Due to the

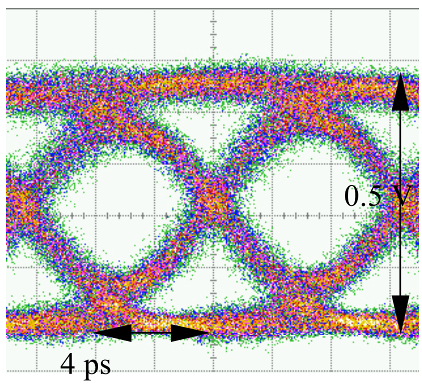

Fig. 5 Detected eye pattern under 160 Gbit/s RZ excitation, V_{bias} = -2.5 V.

insufficient bandwidth of the sampling head (70 GHz, Agilent 86118A) and the PD module we observe an RZ-to-NRZ conversion. Nevertheless, the eye amplitude is still remarkable and the inner eye opening reaches 160 mV.

2. Photoreceivers for 80/85 Gbit/s Applications

The concept of combining a waveguide-integrated photodiode with a spot-size converter and a HEMT-based amplifier and allowing the independent optimization of each of the components has been widely discussed in earlier publications [6, 7]. For 80/85 Gbit/s system applications a circuit design has

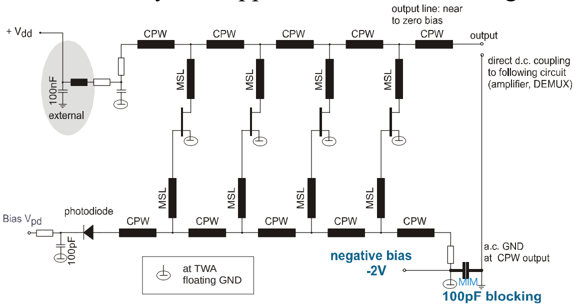

Fig. 6 Circuit diagram of the photoreceiver with negative bias and GND-isolated output port.

been developed, using HEMTs with modified layer structures and shorter gate lengths. The biasing configuration is accomplished with a negative bias supply at the common source electrode blocked with an MIM capacitor [8]. The circuit diagram of the photoreceiver with a negative bias and ground (GND)-isolated output port is depicted in Fig. 6.

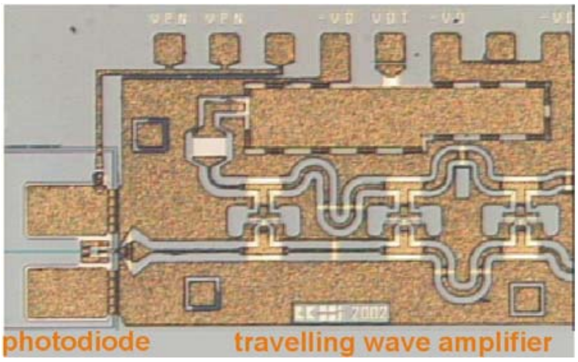

Fig. 7 Partial view of the integrated photoreceiver OEIC.

The amplifier's DC current is fed into the terminal V_{dd}. The HEMTs with 0.18 µm gate length, exhibit cut-off frequencies f_T/f_{max} of typically 140/300 GHz. The complete circuit was designed applying the ADS simulation tool, revealing a minimum 3-dB bandwidth of 65 GHz and transimpedance (Z_T) of 40 dBΩ. The reflection coefficient S_{22} is less than 10 dB over almost the whole frequency range up to 80 GHz. A partial view of the chip is given in Fig. 7, which shows the photodiode at the left being connected to the input of the traveling wave amplifier via an air bridge. The amplifier characteristics defined by the transimpedance (Z_T) is derived from the measured S-parameters. The transimpedance amounts to 39 dBΩ (71Ω) and has a bandwidth of 72 GHz. The packaged photoreceiver is shown in the inset of Fig. 8, with 1 mm RF output, a DC supply and an optical input. The frequency characteristic of the module is given in Fig. 8. The 3 dB bandwidth exceeds 70 GHz, which is comparable to the OEIC characteristics and proves a high quality RF

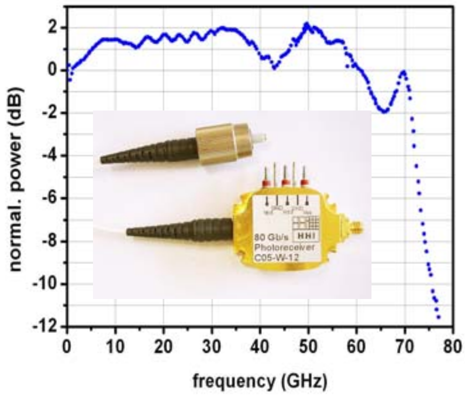

Fig. 8 Opto-electronic frequency response of the pinTWA photoreceiver module: inset: photograph of a pig-tailed OEIC module with 1mm RF output.

packaging. The overall conversion gain of the photoreceiver module is 45.4 V/W, which is high enough for 80 Gbit/s ETDM systems as well as a high frequency measurement equipment. Time domain measurements with the module demonstrated

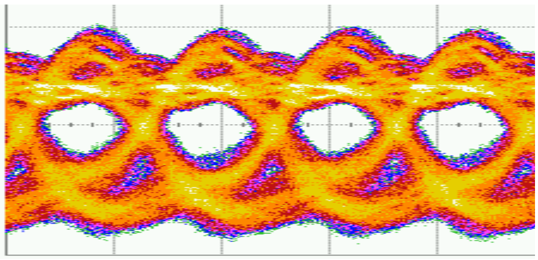

Fig. 9 85 Gbit/s NRZ eye pattern at +7 dBm optical input power detected by the pinTWA receiver module, Alcatel SEL AG, Stuttgart [10], x: 10 ps/div, y: 100 mV/div.

well opened 80 Gbit/s RZ and 85 Gbit/s NRZ eye patterns at 7 dBm optical input power [9, 10]. The back-to-back 85 Gbit/s NRZ eye pattern measurement (Fig. 12) was achieved at +7 dBm optical input power in an ETDM very short range transmission setup at Alcatel SEL AG [10].

3. Transmitter Chip Aiming at THz Applications

Photomixing has proved to be a versatile and convenient measurement technique in the THz frequency range, appropriate to different THz sensor and security applications. The present work focusses on the realisation of an optical-waveguide coupled p-i-n photomixer integrated with a broad-band THz antenna in a single chip, Fig. 10. The broad-band logarithmic-periodic circularly-toothed planar antenna

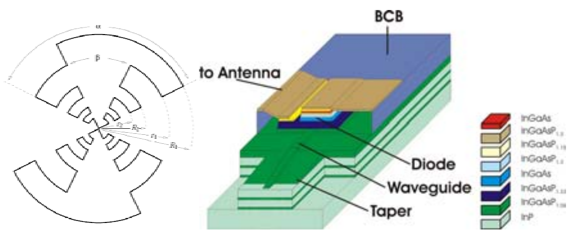

Fig. 10 Components of the photonic mixer: left: logarithmic-periodic circularly-toothed planar antenna, right: schematic view of the waveguide integrated micro-pin photodiode of 5x7 µm^2 size with spot size converter.

allows to cover a wide frequency range from 0.1 to 1.5 THz with a single chip [11]. The optical-waveguide taper implemented in our chip relaxes the tolerances for fibre-coupling by an order of magnitude compared to edge-coupled photodiodes and improves the quantum efficiency of the photomixer by an order of magnitude compared to the back-illuminated THz photodiodes. The transmitter chip was fabricated on InP:Fe substrate employing a metal-organic vapour phase epitaxy (MOVPE) epi-

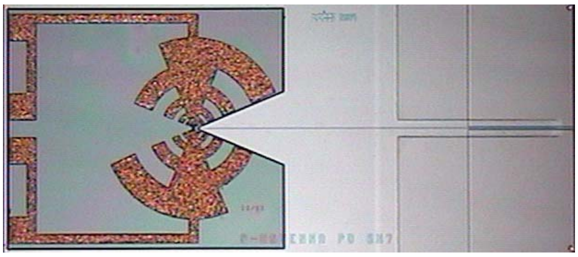

Fig. 11 Photograph of the complete photomixer chip with dimensions 2.75 x 1.4 mm²; illumination is from the right.

taxial approach for the layer stacks of the waveguide-integrated PD. It comprises a spot-size converter, an optical waveguide, a micro p-i-n mesa PD of 5-µm

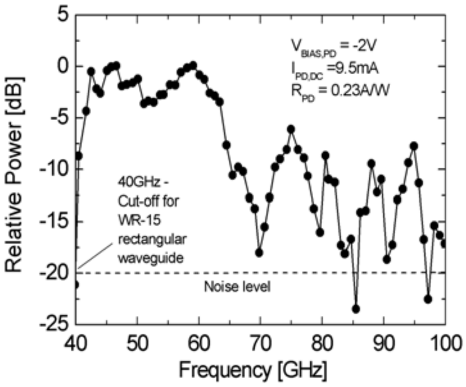

Fig. 12 Heterodyne measured AC characteristics: relative radiated RF output power vs. frequency.

width and 7-µm length [12], and the antenna structure on a BCB layer, cf. to Fig. 11 [13]. The THz signal radiated from the transmitter is received by a special feed horn antenna after free space transfer in a distance of 3 cm above the chip planar side. The detector can transform signals in the frequency range between 10 GHz and 120 GHz. The electrical output signal is measured by a microwave power meter up to –23 dBm. In Fig. 12 the relative power of the electrical signal is plotted versus the beat frequency of the injected optical signal with a power of 15 dBm at a wavelength λ_0 of 1.55 µm. Radiated power measurements applying a lens on the substrate, collecting a quite larger amount of radiated power will be published elsewere.

Conclusions

A highly efficient 100 GHz photodetector module for the detection of single channel bit rates up to 160 Gbit/s RZ has been reported. The detected eye diagrams are well opened with sufficient peak voltages to drive any available demux electronics directly. PinTWA photoreceivers were demonstrated for O/E conversion of 80/85 Gbit/s data rates, applying the RZ/NRZ modulation formats. A prototype of an InP-based integrated THz emitter comprises a micro p-i-n PD with a nominal cut-off frequency of 120 GHz operating as a photonic mixer which determines the maximum frequency of about 100 GHz measured with a feed horn antenna in air above the chips planar side. These results demonstrate the potential of the integration concept of evanescently coupled pin photodiodes for the use in RF microwave links and ultra high-speed systems up to data rates of 160 Gbit/s.

Acknowledgments

The author gratefully acknowledges contributions from his colleagues A. Beling (now ab3pj@virginia.edu), G.G. Mekonnen, R. Gibis, D. Schmidt, R. Kunkel, T. Eckhardt, C. Schubert, W. Ebert, and A. Seeger at the FhI Heinrich-Hertz-Institut, Berlin. Further he acknowledges the cooperation with Alcatel SEL AG, Stuttgart (E. Lach, K. Schuh) and TU Darmstadt (C. Sydlo, P. Meisner). This work was financed partly by the MultiTeraNet program of the German Federal Ministry of Education and Research.

References

1 Y. Muramoto et al, Electron. Lett., 40 (6), pp. 378-379, 2004.
2 A. Beling et al, in Tech. Digest Optical Fiber Communication (OFC 2002), pp. 274–275.
3 A. Beling et al, Electron. Lett., 39 (16), pp. 1204-1205, 2003.
4 H.-G. Bach et al, IEEE JSTQE, Vol. 10, no.4, pp. 668-672, 2004.
5 A. Beling et al, in Tech. Digest Optical Fiber Communication (OFC 2005), paper OFM1.
6 H.-G. Bach et al, Special Issue of IEEE JSTQE, Vol. 2, No. 2, 1996, pp. 418 – 423.
7 W. Schlaak et al, Technical Digest, OFC 2001, Mar 17-22, 2001, Anaheim, CA, USA, paper WQ4, pp. 1-3.
8 G. G. Mekonnen et al, 14th Intern. Conf. on InP and Related Materials (IPRM 2002), May 12-16, 2002, Stockholm, Sweden, paper A8-1.
9 G. G. Mekonnen et al, IEEE JSTQE, Vol. 11, Issue 2, 2005, pp. 356-360.
10 E. Lach et al, 32nd European Conference on Optical Communication (ECOC), 24th-28th September 2006, WP 144.
11 C. Sydlo et al, FREQUENZ, 59, pp. 207-210, 2004.
12 A. Beling et al, IEEE JSTQE, special issue on High-Speed Photonic integration, Vol. 13, No. 1 (2007), pp. 15-21.
13 R. Kunkel et al, Optical Terahertz Science and Technology (OTST), March 18-21, 2007, Orlando, Florida, TuC5.